# TEMPLATE ASSISTED ELECTRODEPOSITION OF HIGHLY ORIENTED ZnO NANOWIRE ARRAYS AND THEIR INTEGRATION IN DYE SENSITIZED SOLAR CELLS

*H. GÓMEZ*, S. CANTILLANA, F.A. CATAÑO, H. ALTAMIRANO. A. BURGOS*

*Instituto de Química. Facultad de Ciencias, Pontificia Universidad Católica de Valparaíso, Av. Universidad 330, Curauma, Valparaíso, Chile.*

## ABSTRACT

Dye sensitized solar cell (DSSC) based on N719 dye sensitized zinc oxide nanowires prepared by template assisted electrodeposition was investigated. The morphology and crystalline structure of highly oriented nanowires were characterized by scannnig electron microscopy and X-ray diffraction, respectively. The photovoltaic performance of the DSSC was characterized at full sun intensity of 100 mW/cm$^2$ obtaining a shortcircuit current of 4.8 mA/cm$^2$, an open circuit voltage of 0.64 V and energy conversion efficiency of 1.23 %.

## 1. INTRODUCTION

During the past decade, nanomaterials have emerged as the new building blocks to design light energy harvesting devices. Organic and inorganic hybrid structures with improved selectivity and efficiency toward catalytic processes have been designed. Size dependent properties in nanoparticles such as quantization effects in semiconductor and quantized charging effects in metals provide the basis for developing new and effective systems[1-8]. These nanostructures provide new strategies for designing next generation energy conversion devices[9-13]. Efforts to synthesize nanostructures with well-defined geometrical shapes have further expanded the possibility of developing new strategies for light energy conversion[14-24].

One of the promising categories is the nanostructured semiconductor base solar cells, particularly the so-called dye sensitized solar cells (DSSCs), currently one of the most efficient and stable excitonic solar cells[25-27]. DSSCs anodes are usually made using thick films (around 10 *μm) of either* $TiO_2$ or, less frequently, ZnO nanoparticles[28-29], which are deposited as a paste and sintered to establish good electrical continuity. The nanoparticle film provides a large internal surface area to allow the anchoring of a sensitizing dye (usually a ruthenium based dye) to produce light absorption in the 400 – 800 nm region. Photons are absorbed by the dye creating excitons (electron-hole pairs) that rapidly split at the nanoparticle film surface. The electrons are injected into the film and holes move to the opposite side of the device through redox species (usually $I^-/I^-_3$ couple) which quickly regenerates the sensitizer.

Particularly, the dye-sensitized cell in which the traditional nanoparticle film is replaced by a dense array of well oriented crystalline ZnO nanowires ensures the rapid collection of carriers generated throughout the device[30]. Compared to mesoscopic semiconductor films, the ordered arrays of either wires and rods provide a well defined architecture. An improvement in the electron transport observed in the ZnO array has been attributed to the decrease in the number of grain boundaries. This approach has been proposed to design ZnO base extremely thin absorber (ETA) solar cells[31].

The choice of ZnO under nanowires form, as an alternative photoanode in DSSCs is justified because the positions of the conduction and valence bands is similar to the $TiO_2$ band positions, but the electron mobility in ZnO is much greater than in $TiO_2$[32]. On the other hand, ZnO is an inexpensive and environmental friendly material that can be synthesized in high purity and crystalline at low temperature. In addition, it can easily grow with different morphologies. Various fabrication techniques have been developed for the growth of ordered ZnO nanowires, such as vapor-liquid–solid growth[33], chemical vapor deposition[34], aqueous solution growth[35], and template based synthesis[36]. Template assisted electrodeposition (TAED), with the use of nanoporous alumina templates, is another alternative well adapted for creating nanostructures of uniform size and well controlled separation between them. It is possible to deposit semiconductors and metals inside the nanoporous alumina and study their electrical and optical properties[37-40]. Furthermore, the use of alumina templates is an economical method for manufacturing large quantities of nanostructures.

TAED appears as a good alternative route to prepare ZnO nanowires that can be potentially used in DSSCs devices. Very important for this purpose is to ensure the optimal carriers collection generated through the device, which is closely related to the crystalline character of the nanowires. Recently, we have successfully accomplished the electrodeposition of ZnO nanowires onto alumina templates, from oxygen and zinc chloride precursors dissolved in dimethylsulfoxide[41]. X-ray diffractograms showed the presence of only one diffraction peak corresponding to the (0002) plane of the ZnO wurzite structure, this is an indication of excellent preferential crystallographic orientation in the c-axis normal to the substrate. Polycrystalline ZnO nanowires embedded in the pores of anodic alumina membrane were also previously electrodeposited by Wang *et. al.* from DMSO solution[42]. They reported a wurtzite polycrystalline structure for the nanowires, stating that the different orientation growth was induced by defects in the wall of the template pores. However, both experimental procedures only differ in that in our case we have not employed KCl as supporting electrolyte. Therefore, chloride concentration plays an important role in the electrochemical ZnO nanowires nucleation-growth mechanism, results which are aligned with those reported in aqueous solution[43].

In current paper highly oriented ZnO nanowires were prepared by TAED on the pores of alumina membranes deposited on ITO (Indium Tin Oxide) substrates from dimethylsulfoxide solutions containing $ZnCl_2$ and $O_2$ as precursors. The nanowires presented a strong crystallographic orientation along the (0002) crystalline planes without any further heating treatment and were assembled as grown as photoanode in a DSSC whose photovoltaic property was tested at full sun intensity of 100 mW/cm$^2$.

## 2. EXPERIMENTAL

ZnO nanowires were grown onto the pores of alumina templates. For this purpose a 1 μm thick aluminum layer was deposited by electron beam evaporation on ITO substrates. Before the anodization process, the aluminum layer was successively rinsed with de-ionized water and dimethyl ketone in an ultrasonic bath. The anodization was performed in a 0.3 M oxalic acid solution applying a voltage of 40 V at 5 $^O$C. To remove the barrier layer and open the pores, the membrane was treated for 20 minutes with a 5 % aqueous $H_3PO_4$ solution at room temperature, followed by 5 minutes of immersion in an aqueous 5% NaOH solution at room temperature. After each chemical treatment the sample was thoroughly rinsed with water and then dried. Figure 1 shows the SEM image of the membrane after pore opening.

The electrodeposition of ZnO nanowires inside the alumina membrane pores was performed in a three electrode electrochemical cell using Ag/$AgCl_{(sat)}$ as reference electrode, a platinum wire as counterelectrode, and the porous alumina membrane onto ITO as working electrode. The electrolytic solution consisted in 0.100 M $ZnCl_2$ and $O_2$ dissolved in DMSO at a fixed potential of -0.8 V and 80°C. Electrodeposition potential was controlled by a Gamry Serie G750 potentiostat. XRD analysis were performed on a Philips PW180 diffractometer (30 kV, 40 mA, CuKα radiation with λ = 1.5406 A°). The diffraction peaks from ZnO and ITO have been indexed by reference to the JCPDS powder diffraction files. The membrane was dissolved with a NaOH

*e-mail address: hgomez@ucv.cl*

solution to get free standing nanowires that were characterized by SEM in a JEOL JSM/5900 LV SEM instrument. N719 dye [cis-diisotiocianato-bis(2,2'-bipiridil-4,4'dicarboxilato)Rutenio(II)bis(tetrabutilamonio), Solaronix] was used as sensitizing agent. To impregnate the dye, the ZnO electrodes were put in a solution of 5 mM of the dye in ethanol at a temperature of 60º−80º C during 30 minutes. A hot-melt adhesive (Dupont surlyn, 25 μm) was sandwiched between the anode and platinised ITO counterelectrode as a spacer. The liquid electrolyte containing 0.2 M of LiI and 0.02 M of $I_2$ was introduced into the space of the two electrodes by capillarity action. The active area of the cell was ca. 0.40 $cm^2$. J-V characterization was made in air using a 1000 W Xenon-Mercury lamp (Oriel 6295) and light intensity of 100 $mW/cm^2$. Current-voltage characteristics of solar cells were recorded by a Keithley 2400 digital sourcemeter.

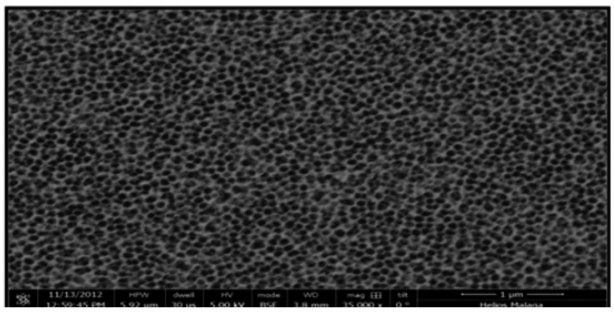

**Figure 1.** SEM Image of the alumina membrane after pores opening.

## 3. RESULTS AND DISCUSSION

### 3. 1 Electrodeposition of ZnO nanowires

Figure 2 shows a typical *J-t* curve corresponding to the electroreduction of oxygen a process that takes places in a bottom-up way starting at the ITO substrate. After an initial abrupt current increasing associated to the double layer charge the current remains stable during the ZnO growing inside the membrane pores.

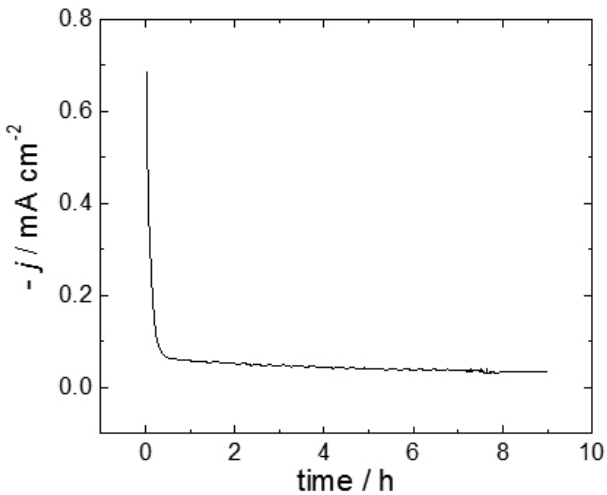


**Figure 2**. j/t typical curve for the bottom-up pore filling.

According to previous studies[44-45], the following mechanism accounts for the electrodeposition of ZnO in DMSO:

$$O_{2(sol)} + e^- \rightarrow O^-_{2(sol)} \quad (1)$$

$$2O^-_{2(sol)} \rightarrow O_{2(sol)} + O^{2-}_{2(sol)} \quad (2)$$

$$O^{2-}_{2(sol)} + Zn^{(II)}_{(sol)} \rightarrow ZnO_{2(s)} \quad (3)$$

$$ZnO_{2(s)} \rightarrow ZnO_{(s)} + \tfrac{1}{2} O_{2(sol)} \quad (4)$$

ZnO formation occurs when the Zn(II) and $O_2^{2-}$ ionic product at the interface reaches a critic value to start with $ZnO_2$ precipitation. As the analysis performed (vide infra) did not show evidences of $ZnO_2$ in the samples, it can be assumed that this compound was completely transformed into ZnO trough step (4).

### 1.2 *Structural and morphological characterization of ZnO nanowire arrays*

In order to study the structural properties of the zinc oxide films, *i.e.*: to investigate the crystallographic phase, the overall crystalline quality of those electrochemically grown thin films, X-ray diffraction analyses were carried out. All XRD peaks (Figure 3) are assigned to the ITO-coated glass substrate (JCPDS 88-0773) and to the hexagonal wurzite phase of ZnO (JCPDS 5-0664). The intensity of the diffraction peaks relative to the background demonstrates a very good crystalline character of the sample. Moreover, no spurious phases were detected by XRD indicating high purity of the hexagonal ZnO phase.

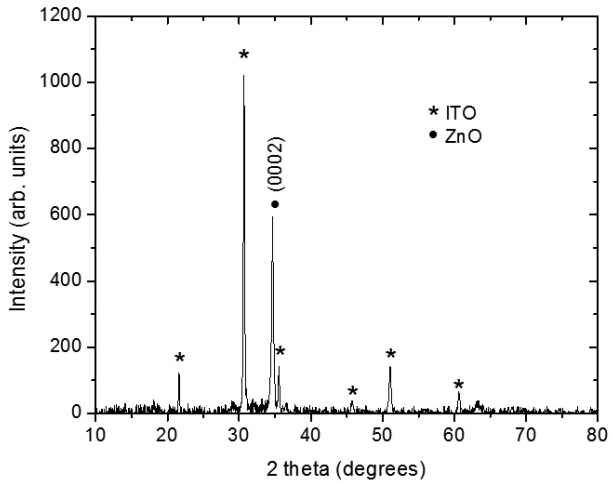


**Figure 3**. XRD difractogramm of as grown ZnO nanowires inside the alumina membrane.

SEM images (Figure 4) show that the layer is homogenous, dense and uniform. The ZnO nanowires appear vertically oriented and well aligned. The average size is 50-60 nm in width and 1 μm in height. The electrodeposited ZnO show only the diffraction peak corresponding to the (0002) plane, which demonstrates that the nanowire grown along the c-axis normal to the ITO substrate.

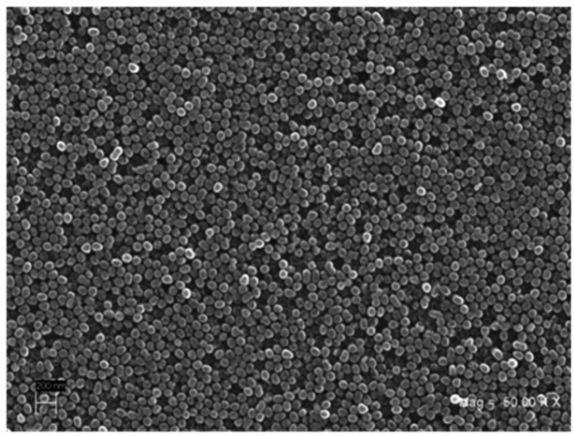

**Figure 4.** SEM image with a top view of free standing ZnO nanowires after membrane dissolution.

### 1.3 Application to dye-sensitized cell

According to previous reports a superior device efficiency is anticipated by replacing the nanoparticles film with a vertical highly oriented nanowire array for enhancing the electron transport rate[46]. The high quality ZnO

nanowire arrays prepared by TAED have been used after sensitization as a photoanode in dye-sensitized solar cells. The N719 dye was chosen due to its compatibility with ZnO in part by a reduced complexing properties for zinc ions. It is important to highlight that depending on the rates of the diffusion of the dye into the nanostructure, adsorption of the dye, dissolution of zinc surface ions and formation of aggregates in the pores of the film, the outer part of the electrode may be in the process of forming aggregates when these processes occurs close to the back contact. This is the reason why it is difficult to avoid dye aggregation completely and the dye treatment need to be optimized in order to get the highest possible solar efficiency.

The *J-V* property of the dye sensitized solar cell with a photoanode formed by a vertically aligned ZnO nanowire arrays is shown in figure 5.

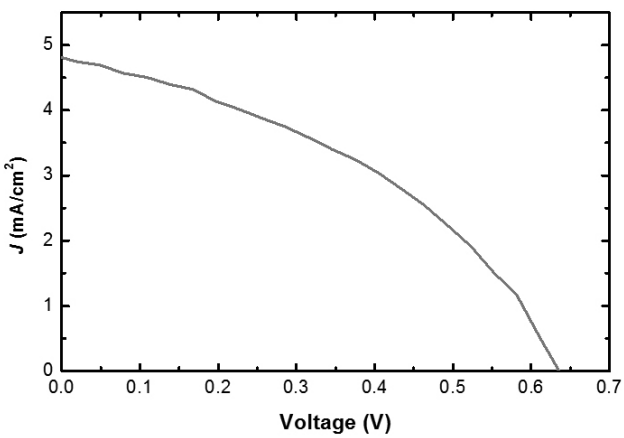


**Figure 5.** *J-V* characteristic for ZnO nanowire arrays sensitized with N719 at full sun intensity of 100 mW/cm$^2$.

The device is characterized by short circuit current of 4.8 mA/cm$^2$, open circuit voltage of $V_{oc}$ = 0.64 V, fill factor FF = 40 % and efficiency η= 1.23 %. The efficiency is similar than the performance reported in the literature for ZnO nanowires photoanodes[47]. Employing mesoporous films of zinc oxide and N719 dye, Chang *et-al* [48] reached 5,61 % of efficiency optimizing the thickness of the oxide film and the dye loading. Efficiencies of 5.55 % [49] and 5.40 % [50] have been reached with the dyes DN350 and CYC-B1 respectively. Comparing our values of open circuit potential and short circuit current with the latter reports, the low efficiency can be attributed to low short-circuit current. Relatively low current can be attributed to interface recombination, low surface area of the nanowires and band loss in ZnO nanowires-based DSSCs due to the uncovered oxide surface (with no dye molecules anchored on).Further work need to be addressed in order to obtain improved efficiencies. The engineering of semiconductor nanowires design morphology may open the possibility of improving the transport of charges and easy filling with solid hole conductors. The use of a simplified geometry as that provide by TAED of nanowires is a clear mean for a better understanding of this type of devices.

## 4. CONCLUSIONS

Highly oriented ZnO nanowires with c-axis preferred orientation were successfully synthesized using template assisted electrodeposition. These nanowires showed suitable properties regarding solar energy conversion application. Owing to their superior electron transport property, the performance of a ZnO-nanowire DSSC gave a remarkable improvement in the open circuit voltage and an acceptable shortcircuit current. The properties of the TAED of ZnO nanowires prove to be good which makes this method promising for future applications.

## ACKNOWLEDGEMENTS

The financial support of FONDECYT, grant 1110619, is gratefully acknowledged. F.A. Cataño acknowledges CONICYT for the doctoral fellowship awarded.

## REFERENCES

1. A. Henglein, *Chem. Rev*. **89**, 1861, (1989).
2. M.L. Steigerwald, L.E. Brus, *Acc. Chem. Res*. **23**, 183, (1990).
3. L. Brus, *J. Phys. Chem*. **90**, 2555, (1986).
4. H. Weller, *Adv. Mater*. **5**, 88, (1993).
5. L. Banyai, S.W. Koch, *Semiconductor quantum Dots*, World Scientific Publishing Co, New Jersey, 1993.
6. K.D. Karlin, P.V. Kamat, Native and surface modified semiconductor nanoclusters*,* Progress in Inorganic Chemistry Series, Meyer, J. Ed. John Wiley & Sons, Inc, New York, (1997).
7. A.P. Alivisatos*, J. Phys. Chem. B*. **100**, 13226, (1996).
8. P.V. Kamat, *J. Phys. Chem. B*. **106**, 772, (2002).
9. D.M. Adams, L. Brus, C.E.D Chidsey, S. Creager,C. Cruetz, C.R. Kagan, P.V. Kamat, M. Lieberman, S. Lindsay, R.A. Marcus, R.M. Metzger, M.E. Michel-Beyerle, J.R. Miller, M.D. Newton, D.R. Rolison, O. Sankey, K.S. Schanze, J. Yardley, X. Zhu, *J. Phys. Chem. B*. **107**, 6668, (2003).
10. K.G. Thomas, P.V. Kamat, *Acc. Chem. Res*. **36**, 888, (2003).
11. A.N. Shipway, E. Katz, I. Willner, *Chem. Phys. Chem*. **1**, 18, (2000).
12. I. Willner, E. Kaganer, E. Joselevich, H. Durr, E. David, M.J. Gunter, M.R. Johnston, *Coord. Chem. Rev*. **171**, 261, (1998).
13. M.D. Ward, *Chem. Soc. Rev.* **26**, 365, (1997).
14. M.A. El-Sayed, *Acc. Chem. Res.* **34**, 257, (2001).
15. C. Burda, X. Chen, R. Narayanan, M.A. El-Sayed, *Chem. Rev.* **105**, 1025, (2005).
16. D.J. Sirbuly, M. Law, H. Yan, P. Yang, *J. Phys. Chem. B.* **109**, 15190, (2005).
17. D. Zheng, S. Sun, W. Fan, H. Yu, C. Fan, G. Cao, Z. Yin, X. Song, *J. Phys. Chem. B.* **109,** 16439, (2005).
18. K.L. Kelly, E. Coronado, L.L. Zhao, G.C. Schatz, *J. Phys. Chem. B.* **107**, 668, (2003).
19. R. Jin, Y.C. Cao, E. Hao, G.S. Métraux, G.C. Schatz, C.A. Mirkin, *Nature.* **425**, 487, (2003).
20. J. Henzie, K.L. Shuford, E.S. Kwak, G.C. Schatz, T.W. Odom, *J. Phys. Chem. B.* **110**, 14028, (2006).
21. C.J. Murphy, A.M. Gole, S.E. Hunyadi, C.J. Orendorff*, Inorg. Chem.* **45**, 7544, (2006).
22. F. Wang, A. Dong, J. Sun, R. Tang, H. Yu, W.E. Buhro, *Inorg. Chem.* **45**, 7511, (2006).
23. L.E. Greene, B.D. Yuhas, M. Law, D. Zitoun, P. Yang, *Inorg. Chem.* **45**, 7535, (2006).
24. T.R. Kline, M. Tian, J. Wang, A. Sen, M.W.H. Chan, T.E. Mallouk, *Inorg. Chem.* **45**, 7555, (2006).
25. B.A. Greg, J. Phys. Chem. B. **107**, 4688, (2003).
26. M.K. Nazeeruddin, P Péchy, T. Renouard, S.M. Zakeeruddin, R. Humphry-Baker, P. Comte, P. Liska, L. Cevey, E. Costa, V. Shklover, L. Spiccia, G.B. Deacon, C.A. Bignozzi, and M. Grätzel, *J. Am. Chem. Soc*. **123**, 1613, (2001).
27. P. Wang, S.M. Zakeeruddin, J.E. Moser, M.K. Nazeeruddin, T. Sekiguchi, M. Grätzel, *Nat. Mater*. **2**, 402, (2003).
28. K. Tennakone, G.R.R.A. Kumara, I.R.M. Kottegoda, V.P.S. Perera, *Chem. Commun.* **1**, 15, (1999).
29. K. Keis, E. Magnusson, H. Lindstrom, S. Lindquist, A. Hagdfelt, *Sol. Energ. Mater. Sol. Cells*. **73**, 51, (2002).
30. J. Nissfolk, K. Fredin, A. Hagfeldt, G. Boschloo, *J. Phys. Chem. B*. **110**, 22950, (2006).
31. C. Levy-Clément. Nanostructured Materials for Solar Energy Conversion, T. Soga Ed. Elesevier (2006).
32. Y. Li, W. Xie, X. Hu, G. Shen, X. Zhou, Y. Ziang, X. Zhao, P. Fang, *Langmuir*. **26**, 591, (2010)
33. M.H. Huang, S. Mao, H. Feick, H. Yan, Y. Wu, H. Kind, E. Weber, R. Russo, P. Yang, *Science*. **292**, 1897, (2001).
34. W.I. Park, D.H. Kim, S.W. Jung, G.C. Yi, *Appl. Phys. Lett.*, **80**, 4232 (2002).
35. L. Vayssieres, K. Keis, S.E. Lindquist, A. Hegfeld, *J. Phys. Chem. B*. **105**, 3350, (2001).
36. Y. Li, G.W. Meng, L.D. Zang, *Appl. Phys. Lett*. **76**, 2011 (2000).
37. A. Cortés, G. Riveros, J.L. Palma, J.C. Denardin, R.E. Marotti, E.A. Dalchiele, H. Gómez, *J. Nanosci. and Nanotech*. **9**, 1992, (2009).
38. G. Riveros, J. Vásquez, H. Gómez, T. Makarova, D. Silva, R.E. Marotti, E.A. Dalchiele, *Appl. Phys. A*. **90**, 423, (2008).
39. S. Green, A. Cortés, G. Riveros, H. Gómez, E.A. Dalchiele, R.E. Marotti, *Phy. Stat. Sol. C*. **4**, 340, (2007).

40. E.A. Dalchiele, R.E. Marotti, A. Cortes, G. Riveros, H. Gómez, L. Martínez, R. Romero, D. Leinen, F. Martin, J.R. Ramos-Barrado, *Phys E*. **37**, 184, (2007).
41. H. Gómez, G. Riveros, D. Ramirez, R. Henríquez, R. Schrebler, R.E. Marotti, E.A. Dalchiele, *J. Solid. State. Electrochem*. **16**, 197, (2012).
42. Q. Wang, G. Wang, B. Xu, J. Jie, X. Han, G. Li, Q. Li, J.G. Hou, *Mater. Lett.* **59**, 1378, (2005).
43. R. Tena-Zaera, J. Elías, G. Wang, C. Lévy-Clement, *J. Phys. Chem. C*. **111**, 16706, (2007).
44. R. Henriquez, M. Froment, G. Riveros, E.A. Dalchiele, H. Gomez, P. Grez, D. Lincot, *J. Phys. Chem. C*. **111**, 6017, (2007).
45. R. Henriquez, H. Gomez, P. Grez, D. Lincot, M. Froment, E.A. Dalchiele, G. Riveros, *Electrochem. Solid-State Lett*. **10**, D134, (2007).
46. M. Law, L.E. Green, J.C. Johnson, R. Saykally, P. Yang, *Nat. Mater*. **4**, 445, (2005).
47. O. Lupan, V.M. Guérin, I.M. Tiginyanu, V.V. Ursaki, L. Chow, H. Heinrich, P. Pauporté, *J. Photochem. Photobiol. A*. **211**, 65, (2010).
48. W.C. Chang. C.H. Lee, W.C. Yu, C.M. Lin, *Nanoscale Res. Lett.* **7**, 688, (2012).
49. S. Higashijima, Y. Inoue, H. Miura, Y. Kubota, K. Funabiki, T. Yoshida, M. Matsumi, *RCS Adv.* **2**, 2721, (2012).
50. C.P. Lee, C.Y. Chou, C.Y. Chen, M.S. Yeh, L.Y. Lin, R. Vittal, C.G. Wu, K.C. Ho, *J. Power Sources*. **246**, 1, (2014).